Rhodium-based cathodes with ultra-low metal loading to increase the sustainability in the hydrogen evolution reaction

Gema Pérez [a], Guillermo Díaz-Sainz [a], Lucía Gómez-Coma [a], Lucía Álvarez-Miguel [b], Aymeric Garnier [b], Nolwenn Cabon [c], Alfredo Ortiz [a], Frederic Gloaguen [b], Inmaculada Ortiz [a,*]

[a] Departamento de Ingenierías Química y Biomolecular, Universidad de Cantabria, Avenida de los Castros 46, Santander 39005, Spain
[b] UMR 6521, CNRS, Université de Bretagne Occidentale, CS 93837, Brest 29238, France
[c] UMR 6226, CNRS, Université de Rennes 1, Campus Beaulieu, Rennes 35042, France

ABSTRACT

Climate change mitigation is one of the main global challenges in the 21st century. In this context, the recent 26th United Nations Climate Change Conference of the Parties (COP26-Glasgow) claimed for searching urgent and efficient measures to reduce and ultimately avoid CO_2 emissions. Thus, many efforts from the scientific community focus on the research of new and renewable energy sources (RES). Among other approaches, green hydrogen, which comes from water electrolysis, is a promising candidate to be considered in the energy panorama. However, commercial electrolyzers are provided with Pt/C and Ir-based electrocatalytic materials, which are expensive and not abundant, to catalyze the Hydrogen Evolution Reaction (HER) in safe, stable, inexpensive, and environmentaly friendly conditions. Thus, this work aims to synthesize high-performance and very low metal loading catalysts by immobilizing a Rh-based organometallic complex (RhCp*Cl(phendiamine))Cl) on a carbon black support following a robust synthesis procedure. Advanced characterization of the synthesized materials confirmed that ultra-low metal loadings in the range of 3.2–4.7 mg·g^{-1} were successfully reached. Subsequently, Rh-based catalysts were tested in a PEM electrolyzer. For metal loadings as low as 0.0066 mg·cm^{-2} competitive cell potentials of 1.9 V were achieved working with 0.5 A·cm^{-2} geometric current density at 70 °C. These results are comparable to those obtained with Pt-based commercial cathodes working under similar operation conditions. Thus, the results of this research make a step forward in the substitution of conventional cathodes for the electrolytic HER by new materials with very low metal loadings.

1. Introduction

The continuous emissions of greenhouse gases resulting from the combustion of fossil fuels pose a threat to the Earth due to its influence on climate change. The negative impact on natural resources and health requires urgent actions to mitigate an imminent disaster [1,2]. In this context, the recent Conference of the Parties (COP26) held in Glasgow (Scotland), from 31 October to 13 November 2021, claimed to reduce CO_2 emissions by 45% in 2030 to limit an increase in the global average temperature of 1.5 °C with respect to the pre-industrial period. Thus, searching for new greener alternatives to substitute the current energy sources is crucial to achieve the targets imposed by COP26 [3]. Among other sustainable energy options, hydrogen appears as an ideal candidate since this energy carrier is considered as a zero-emission fuel that promotes a green world, as it delivers clean power and leads to the

formation of water as the only by-product of its conversion to electrical energy [4–6].

Currently, natural gas reforming is the most common method for hydrogen production [7,8] but there are other emerging methods available, like partial oxidation of hydrocarbons [9], chemical decomposition [10,11], coal or biomass gasification [12], photocatalysis [13–15] or electrolytic processes [4,6,16]. The electrolytic water splitting, is considered the greenest hydrogen obtention route so far as it avoids any direct carbon emissions when electrolyzers are powered by renewable sources [16-20].

In this context, Proton Exchange Membrane (PEM) electrolyzers report a number of advantages such as high current densities and voltage efficiencies, good partial load range, rapid system response, compact system design, and reasonable gas purity [4,21,22]. However, the main drawback of PEMs is the use of platinum to catalyze the hydrogen

---

* Corresponding author.
E-mail address: ortizi@unican.es (I. Ortiz).

evolution reaction (HER) and, also platinum or iridium-based materials to carry out the oxygen evolution reaction (OER); both metals are expensive and not abundant materials [21,23,24]. Thus, finding alternative electrocatalysts that are cost-effective while maintaining the performance of the latter electrodes becomes a priority for implementation at industrial scale [25–27].

The performance of HER in electrochemical water splitting is usually studied by the analysis of the behavior of new electrocatalysts [4,21]. Precious metals different from Pt, such as Au, Pd, or Ag, were first considered as promising electrocatalysts but they are also expensive and not abundant, inhibiting their practical application at the industrial scale [24]. Another approach widely studied in literature is the use of non-noble metals, such as Mo, Ni, Co, Cu, Fe, and W, that appear as good candidates, due to their inherent properties, like lower price, good catalytic performance in the acid electrolyte, and excellent catalytic stability [4,16,28]. However, the electrocatalysts reported in the literature so far require high metal loadings ($0.5 - 1$ mg·cm^{-2}) to achieve similar performance to those obtained with Pt-based electrocatalyts [21,23]. Therefore, and to overcome this challenge, several authors proposed a rational design of electrocatalysts with low metal loading and high metal utilization.

In the last few years, transition metal carbides, phosphides and chalcogenides have received extensive interest, in the development of non-noble metal-based electrocatalysts to carry out the HER [29]. For example, molybdenum carbide has demonstrated similar catalytic properties as noble metals (i.e. Pt). Consequently, many scientists focus the research on developing molybdenum carbides as effective electrocatalysts for hydrogen production [30]. Moreover, Mo-based catalysts are recognized as an affordable alternative [25], e.g. $CoMoS_2$ reached current density values similar to those achieved by commercial 20% wt. Pt/C cathode under industrially applicable conditions.

Besides, Holzapfel et al. [31] reported remarkable values of current density of 1 A·cm^{-2} during 100 h, when Mo_3S_{13} is supported on nitrogen-doped carbon nanotubes. On the other hand, Ni, which favors the HER performance, is commonly used as alloys, like NiMo, NiCo, NiCu, and in ternary metal mixtures (e.g. NiMoZn) [24]. Shi et al. [32] also synthesized electrocatalysts based on $Ni_{12}P_5$-Ni_2P heterostructures, through a cost-effective and easy to implement method, and reported high HER performance, with an overpotential value of 166 mV at 10 mA cm^{-2}, and many active sites for hydrogen generation, exhibiting long term durability in a single cell PEM electrolyzer. Cobalt oxides have also received considerable attention as promising HER electrocatalysts [24]. However, it is essential to improve the electrical conductivity of these metal oxides through the introduction of carbon nanotubes (CNTs), graphene, metal foam, or carbon cloth. In this sense, $Co_{59}Cu_{41}$ was shown to be a suitable electrocatalyst for the HER, exhibiting excellent durability and excellent performance with an overpotential of 342 mV at 10 mA cm^{-2} [22]. Finally, most of the research studies have been mainly focused on decreasing electrocatalysts loadings and operational costs by increasing the specific performance and durability of the electrocatalysts by using carbon-supported materials, consisting of earth-abundant materials, such as Ni-C, Mo_2C/CNTs, Ni_2P/CNTs, Co-doped FeS_2/CNTs, or WO_2/C [23].

Other non-metals, such as B, C, N, P, S, or Se, have been tested in the synthesis of HER electrocatalysts [28]. In this context, Shiva-Kumar et al. [33,34] synthesized boron-doped carbon nanoparticles (BCNPs) achieving stable performances in PEM cells. Finally, noble metals like Ir, Ru, and Rh showed outstanding catalytic performance for the HER [28, 29,35]. Previous works demonstrated that the use of Ir-based materials promote the HER kinetics [36]. On the contrary, other authors, to accomplish inexpensive PEM electrolysis methods, developed alternative electrocatalysts, based on low-cost Ru-based multi-metallic oxides improving at the same time the efficiency and stability of the system [23]. In this way, a significant number of studies presented Ru-based catalyst as a valuable material for HER in water electrolysis exhibiting similar intrinsic activity as for Pt and possessing the merits of relatively low cost and excellent durability. For example, graphene-supported ruthenium telluride nanoparticles ($RuTe_2$/Gr) have been demonstrated as suitable and easily fabricated catalyst, and with excellent catalytic stability and low cost [16]. The high catalytic performance showed by $RuTe_2$/Gr is attributed to its high dispersion on the graphene surface, high electrical conductivity, and low charge transfer resistance. On the other hand, Sarno and Ponticorvo, produced new electrocatalysts based on RuS_2 nanoparticles covered by small edge size MoS_2 nanosheets, obtaining a RuS_2@MoS_2 cathode for a PEM electrolyzer, evidencing a good behavior with Tafel slopes of 36 mV·dec^{-1} and negligible overpotentials [37]. Paunović et al. [38] studied the electrocatalytic activity of mixtures of Co-Ru deposited on activated multiwalled carbon nanotubes (MWCNTs) in PEM electrolyzers, ranging the catalytic activity for HER as follows: CoRuPt (4:0.5:0.5) > CoPt (1:1) > Pt > CoRu (1:1) > CoRu (4:1).

On the other hand, Rh appears also as an excellent electrocatalyst in a wide pH range and with promising applications in hydrogen generation and hydrogenation reactions [39]. Bai et al. [40] synthesized bimetallic PtRh alloy nanodendrites and reported higher electrocatalytic activity in comparison with monometallic Pt nanocrystals, enhancing the reaction rate of ethanol oxidation in direct alcohol fuel cells. Adequate performance for the methanol oxidation reaction in alkaline media fuel cells were reported by Kang et al. [41] using rhodium nanosheets on reduced graphene oxide. However, Rh-based electrocatalysts have rarely been reported for water splitting reactions, and specifically in acid media. Within the most representative works focused on the use of Rh-based catalysts, Han et al. [39] and Lu et al. [42] reported that alloying platinum with rhodium might cause an increase in the catalytic activity for the HER in comparison to platinum alone. Besides, ultrathin RhCo alloy and Rh-Rh_2O_3 nanoparticles nitrogen-doped carbon composites (Rh-Rh_2O_3-NPs/C) were synthesized and their electrocatalytic performance for water splitting in acid, neutral and alkaline solutions exhibited higher activity and long term stability than Pt-based electrocatalysts [43,44]. Finally, monodisperse rhodium phosphide nanocubes (Rh_2P NCs), revealed an extraordinary catalytic performance for HER in acid media, although further investigation on the reaction mechanism is needed [45].

The literature review presented above clearly shows that the electrodes in PEM electrolyzers are usually fabricated from metal nanoparticles to increase the number of active sites per unit of geometric surface area, and thus the current density while decreasing the overall metal loading and the process cost. Considering that the lowest achievable size for an active site is a single metal atom, the development of single-atom catalysts (SACs) has recently emerged as a powerful approach to maximize the use of precious metals while boosting the electrocatalytic performance [46]. For example, SACs made of Pt traces deposited on nitrogen-doped graphene were reported to achieve promising performance for the HER [47]. On the other hand, immobilization of organometallic complexes on suitable supports offers the prospect of synthesizing heterogeneous catalysts in which the chemical environment of the metal site is well-controlled and remains well-defined [48].

Recently, Surendranath et al. [49] have reported a novel class of materials in which a transition metal-based molecular catalyst is electronically coupled to a smooth oxidized graphite surface by means of a pyrazine link, leading to a metal-like electrocatalytic behavior. Besides, Gullá et al. [50] prepared various Rh_xS_y loadings on carbon black powder for the electrolysis of hydrochloric acid, demonstrating that it is possible to reduce efficiently and effectively the precious metal loading without affecting the cell performance or the catalyst durability.

The main goal of the present work is to synthesize high-performance electrocatalysts with very low metal loadings by immobilizing a Rh-based organometallic complex on carbon black powder (Vulcan XC-72) and comparatively assess the behavior of this electrocatalysts for the HER. The Rh-complex/Vulcan XC-72 (Rh/C) electrocatalyst has been characterized by proton nuclear magnetic resonance (^{1}H NMR), UV–vis spectroscopy, and inductively coupled plasma-mass

spectrometry (ICP-MS), and its behavior for the HER is investigated by experiments in a rotating disk electrode (RDE) in an aqueous acidic electrolyte. Finally, its electrocatalytic activity for the HER is evaluated by preparing Gas Diffusion Electrodes as cathodes in a single cell PEM electrolyzer and the results are compared with those obtained with precious Pt commercial materials with high metal loading.

2. Methodology

This section collects the materials and methods used for the immobilization of Rh-based organometallic catalysts on carbon black powder, the RDE measurements, as well as the description of both the laboratory PEM electrolyzer cell and the testing protocol. Besides, detailed information about the synthesis of the Rh/C electrocatalysts and part of the characterization are incorporated as Supplementary Information (SI).

2.1. Synthesis of Rh/C electrocatalyst

[RhCp*Cl(phendiamine)]Cl (Cp* = pentamethylcyclopentadienyl, phendiamine = 5,6-diamino-1,10-phenanthroline) was synthesized by adapting a preparation method previously described in the literature [51]. This Rh complex was then grafted on chemically oxidized Vulcan XC-72 powder through a pyrazine link (Fig. 1) by modifications of the procedure described by Surendranath et al. [49]. Complete details of the preparation of 5,6-diamino-1,10-phenanthroline, [RhCp*Cl(phendiamine)]Cl and Rhodium complex/Vulcan XC-72 (Rh/C) electrocatalyst are provided in the Supplementary Information.

2.2. Physical characterization of Rh/C electrocatalyst

The Rh complex and Rh/C electrocatalyst have been characterized by ^{1}H NMR, UV–vis spectroscopies, and inductively coupled plasma-quadrupole mass spectrometry.

Firstly, proton NMR spectra were recorded with a 400 MHz Bruker Advance spectrometer. All chemical shifts (δ) values are given in parts per million (ppm) relative to tetramethylsilane as an external reference, and on the other hand, all coupling constants (J) are quoted in Hz. On the other hand, the UV–vis spectra were recorded in a 10 mm quartz cuvette using a Perkin-Elmer Lambda 25 spectrometer. Moreover, measurements of the Rh concentrations (^{103}Rh isotope) in the Rh/C electrocatalyst were conducted on diluted mixtures (2.6% HNO$_3$) by using an inductively coupled plasma-quadrupole mass spectrometer (X-series II, Thermo Scientific) with a H$_2$ collision cell. Digestion of the Rh/C samples (10 mg) was conducted at 105 °C for 4 h in a closed Teflon screw-cap vial (30 mL, Savillex) with 1 mL HNO$_3$ (65% wt., Merck suprapur) and 0.25 mL H$_2$O$_2$ (30% wt. Merck suprapur). Three Rh standard solutions were used (i.e. 11.74, 2.384, and 0.4443 mg L^{-1}). These solutions, also in 2.6% HNO$_3$, were prepared from a 1000 mg L^{-1} stock solution (Sigma Aldrich). For each step (powder weighing, addition of nitric acid and hydrogen peroxide solutions, sample dilution, and

standard preparations) a Kern ABT-120 balance with a precision of 0.01 mg was used to accurately calculate the Rh concentrations in the standards and samples.

In addition, surface characterization was also performed by high angle annular dark field scanning transmission electron microscopy (HAADF-STEM), and X-ray Photoelectron Spectroscopy (XPS). In the case of HAADF-STEM, the measurements were obtained using the Titan Themis G2–60–300 microscope equipped with an Energy Dispersive X-Ray Spectroscopy (EDS) system for chemical composition analysis, and a rapid camera at 4 K X 4 K resolution at 300 kV. Moreover, XPS measurements were performed in a SPECS system (Germany) equipped with a Phoibos 150 1D-DLD analyzer and monochromatic Al Kαα radiation source (1486.7 eV). Finally, images and composition analysis of the Rh/C catalyst were acquired with a scanning electron microscope (SEM) HITACHI S-3200 N equipped with an energy-dispersive X-ray (EDX) spectrometer Princeton Gamma-Tech.

2.3. Electrochemical characterization of Rh/C electrocatalyst

The rotating disc electrode (RDE, surface area of 0.071 cm^2) tip was constructed from a glassy carbon (GC) disk (0.3 cm in diam.) embedded in a Teflon rod (1 cm in diam.). The GC disk was coated with a thin film of Rh/C electrocatalyst supported in Nafion following the procedure described by Gloaguen et al. [52]. Briefly, measured amounts of Rh/C powder (50 mg), with a known Rh loading, Nafion solution (5% in wt.) in isopropanol (1 g), and MilliQ water (5 mL) were sonicated using an ultrasonic bath. A measured volume (ca. 2 µL) of the resulting ink was dropped over the GC disk and set to dry at room temperature (18 ± 1 °C). The Rh/C in Nafion film thus formed was rinsed with water and equilibrated in a 0.1 M H$_2$SO$_4$ aqueous solution for several hours. The thin film-coated RDE (1 µm of thickness) was then placed in a glass cell also equipped with a graphite rod and a Hg/HgSO$_4$ electrode (MSE) used as a counter electrode and as a reference electrode, respectively. The potentials were converted to the reversible hydrogen electrode (RHE) scale using Eq. (1):

$$E(vs\ RHE) = 0.66V + 0.06V \cdot pH \tag{1}$$

The recorded currents were not corrected for the ohmic drop, which was anticipated to be negligible under our experimental conditions.

2.4. Rh/C-GDE fabrication

The assessment of the performance of the Rh/C electrocatalyst, that had been synthesized and characterized previously, was carried out in a commercial electrolyzer. A Rh/C-Gas Diffusion Electrode (Rh/C-GDE) was fabricated to be used as cathode. For this purpose, a porous titanium Gas Diffusion Layer (GDL), with a porosity and thickness of 45% and 1 mm, respectively, supplied by H2Greem Global Solutions was used as the electrocatalyst support, in which the Rh/C electrocatalyst was
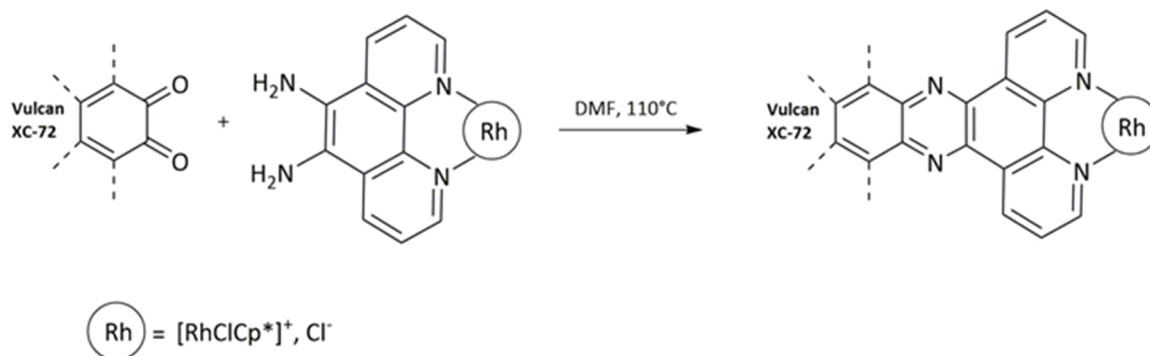

Fig. 1. Grafting of the Rh complex on oxidized carbon black powder (Vulcan XC-72) through the formation of a pyrazine link.

directly deposited following the catalyst-coated substrate (CCS) method and applying the airbrushing technique. The total geometric surface area of the Rh/C-GDE was 25 cm^2.

Before depositing the electrocatalyst layer into the GDL, it was cleaned by boiling first in isopropanol and then in ultrapure water. Subsequently, the catalytic layer was air-brushed over the GDL. The catalytic ink was prepared with Rh/C electrocatalyst and Nafion (Nafion™ D2020CS Alcohol based 1000 EW at 20% weight) in a mass ratio of 60/40, and then diluted in isopropanol, (Pharma Grade, Panreac) to obtain a final slurry of 1.9 wt%. The catalytic ink was sonicated for at least 30 min (Bandelin Sonorex Digitec) in a controlled temperature sonicator to ensure uniform mixing. The Rh metal loadings were 0.0044, and 0.0066 mg·cm^{-2}, respectively.

2.5. Electrolyzer tests

The Rh/C-GDEs were then used to catalyze the hydrogen evolution reaction at the cathode in a commercial PEM electrolyzer (Hart 250 model, Hidrogena Desarrollos Energeticos SI). The main characteristics of this low-pressure hydrogen generator that was equipped with a monocell are summarized in Table 1. A schematic diagram of the internal structure of the monocell is depicted in Fig. 2. Moreover, a power source, water pump, multiple regulation system, hydrogen flowmeter, micro-valve, and multimeter are also integrated in the electrolyzer, completing the experimental setup.

The cathodic and anodic compartments are separated by a proton exchange membrane (PEM) Nafion 115 (IonPower Gmb). The Nafion 115 membrane was pre-treated by soaking it in 3 wt% hydrogen peroxide (H$_2$O$_2$) at 80 °C for 1 h. Subsequently, the membrane was cleaned with ultrapure water and put in a recipient containing hot ultrapure water for 2 h at 80 °C. Then, the membrane was treated with an acidic solution of 0.5 M hydrochloric acid (HCl) at 80 °C for 1 h. Finally, the membrane was rinsed and stored submerged in ultrapure water for its further usage. Moreover, a commercial GDE was used as the counter electrode (H2Greem Global Solutions). This anode was made of an electrocatalyst based on metallic oxides with a loading of 2.5 mg·cm^{-2}.

Finally, the performance for HER of the Rh/C electrocatalyst was compared to other commercial materials. The Rh loading of 0.0066 mg·cm^{-2}, which offers the best performance, was obtained by depositing the same amounts of reactants as those used for Pt-based cathodes. On the one hand, a GDE made of Pt carbon-supported electrocatalysts (CPt/C-GDE) (Platinum on carbon – extend of labeling: 10 wt% loading, matrix activated carbon support, Sigma-Aldrich,) with a loading of 0.3 mg Pt·cm^{-2}, was prepared by following the same procedure as mentioned previously. On the other hand, a commercial MEA (HYDRion, Ion Power GmbH) composed of a Pt loading of 0.3 mg·cm^{-2} (at the cathode side), and Ir-black loading of 1 mg·cm^{-2} (at the anode side) was also tested. Finally, the authors study the behavior of a commercial GDE made of Pt/C (Pt/C-GDE) with a loading of 0.4 mg Pt·cm^{-2} and fabricating also by airbrush technique (20 wt% Pt, H2Greem Global Solutions).

For the study of the performance of the electrolyzer, the polarization curves were measured at atmospheric pressure and controlling the

temperature at values of 50, and 70 °C, for a range of geometric current densities from 0.04 to 0.48 A·cm^{-2}. All experiments were at least triplicated, under the same operating conditions, ensuring that the maximum standard deviations for the replicates of each experimental point were lower than 10% and without evidence of catalyst degradation. Besides, all the experiments were carried out with three different samples of the same electrode to ensure the robustness of our fabrication method. In all the cases, before starting the experiments, the first 30 min were dedicated to stabilizing the system in open-circuit voltage and fixing the value of temperature. Consequently, before data recording, a waiting period of 5 min was spent to confirm the proper hydrogen flow rate and voltage for each value of current density.

3. Results and discussion

3.1. Characterization of the Rh/C electrocatalyst

^{1}H NMR spectra of [RhCp*Cl(phendiamine)]Cl were recorded in DMSO-d6, showing all the chemical shifts in ppm, and the coupling constants are quoted in Hz (Fig. S3 of the Supporting Information). On the other hand, following the recent work of Surendranath et al. [49], we decided to investigate the grafting of a Rh organometallic complex supported on oxidized Vulcan XC-72 by means of a pyrazine link, i.e. by the condensation of the two amine groups of the phenanthroline ligand of the Rh complex with two adjacent carboxyl groups on the carbon surface (see Supplementary Information for experimental details).

To follow the grafting of the Rh complex (Fig. 1), we first recorded the UV–vis absorption spectrum of the mixture in ethanol before and after heating at 60 °C over a period of 6 h, as depicted in Fig. 3. The decrease of the absorbance of the band at $\lambda_{max} = 276$ nm indicates that the concentration of the Rh complex in solution has decreased by ca. 80%, suggesting an efficient grafting. In addition, the UV–vis spectrum recorded after 6 h did not show any new absorption bands, indicating that the Rh complex is stable in solution under the grafting conditions.

Moreover, analysis by an inductively coupled plasma-mass spectrometer (ICP-MS) of six different Rh/C samples gave Rh loadings between 3.2 and 4.7 mg·g^{-1} (see Supplementary Information). The tests in the PEM electrolyzer were carried out with the Rh/C samples exhibiting the highest Rh loadings (i.e. an average value of 4.4 mg·g^{-1}).

Fig. 4 displays a representative HAADF-STEM images of the Rh carbon-supported catalyst. In addition, and to confirm the correlation between the HAADF-STEM intensity profiles and the Rh/C electrocatalyst distribution, EDX-STEM compositional maps for rhodium, oxygen, carbon, and sulphur were taken, as also shown in the mentioned figure. In this sense, the HAADF-STEM and the corresponding element mappings provide the convincing evidence that the Rh complex is distributed over the catalyst structure.

In contrast, XPS measurements were also developed to study the surface chemistry of our material. In this sense, Fig. 5 depicts the XPS spectra of the Rh 3d region. It is observed the presence of two binding energy contributions at 310.3 (Rh 3d 5/2) and 314.8 eV (Rh 3d 3/2) related to Rh^{3+} [53]. In addition, and to provide a complete XPS characterization, Table S1 of the Supplementary Information in the revised version shows the binding energy contribution as well as the relative atomic percentage of each detected element in two samples used to carry out the HER in the PEM electrolyzer. As can be observed in the Table mentioned above, both measurements are nearly identical, demonstrating homogeneity and, therefore, a robust catalyst procedure.

The SEM-EDX spectroscopy, which has a depth analysis of ca. 1 μm, showed the presence of Rh, along with Cl and N, confirming the grafting of the Rh complex (Fig. S5 of the Supplementary Information). The spectra also show, albeit at a low level, the presence of S, which is a well-known contaminant of Vulcan XC72. Besides, SEM image coupled with composition mapping by EDX spectroscopy also show a uniform distribution of Rh, Cl and N over the analyzed sample (Fig. S6).

Table 1

Characteristics of the Hart 250 electrolyzer.

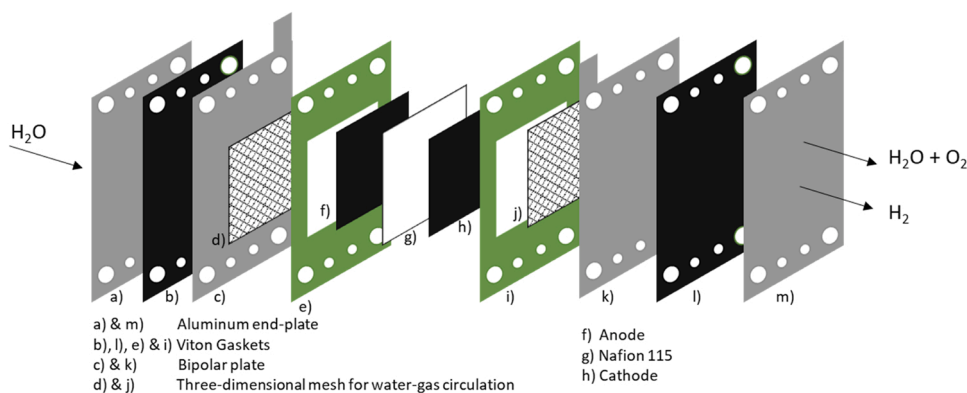|	
Maximum hydrogen production	250 mL·min^{-1}
Maximum hydrogen pressure	12 bars
Hydrogen purity	> 99.9999%
Maximum oxygen production	125 mL·min^{-1}
Electrical consumption	< 100 W
Maximum current density	0.48 A·cm^{-2}
Water Volume	1 L
Water type	deionized ASTM Type II
Dimensions (width x height x depth)	250 × 440 x 340 mm
Empty weight	9 kg

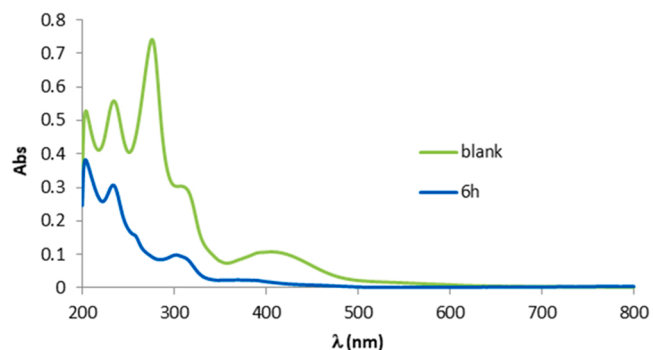**Fig. 2.** Internal structure of the electrolyzer used for hydrogen production.

Fig. 3. UV–vis absorption spectra or a solution of [RhCp*Cl(phendiamine)]Cl in EtOH before (green) and after a reaction with oxidized Vulcan XC-72 over a period of 6 h at 60 °C (blue). The initial concentration of the Rh complex in solution was 1.7×10^{-5} M ($\varepsilon_{Rh} = 142849$ M^{-1} cm^{-1} at $\lambda_{max} = 276$ nm).

3.2. Electrochemical characterization of the Rh/C electrocatalysts

Before evaluation in a PEM electrolyzer, it is important to characterize the properties of the Rh/C electrocatalysts using the RDE setup
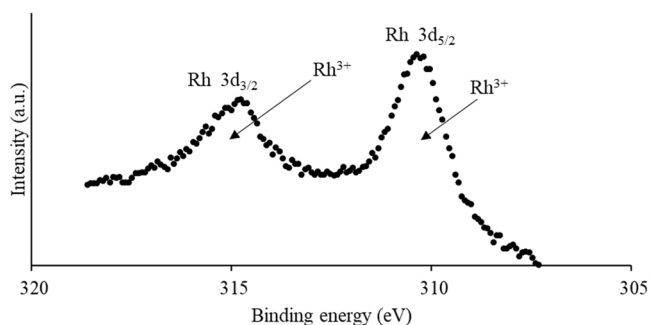
Fig. 5. XPS spectra recorded of Rh 3d region of Rh/C samples.
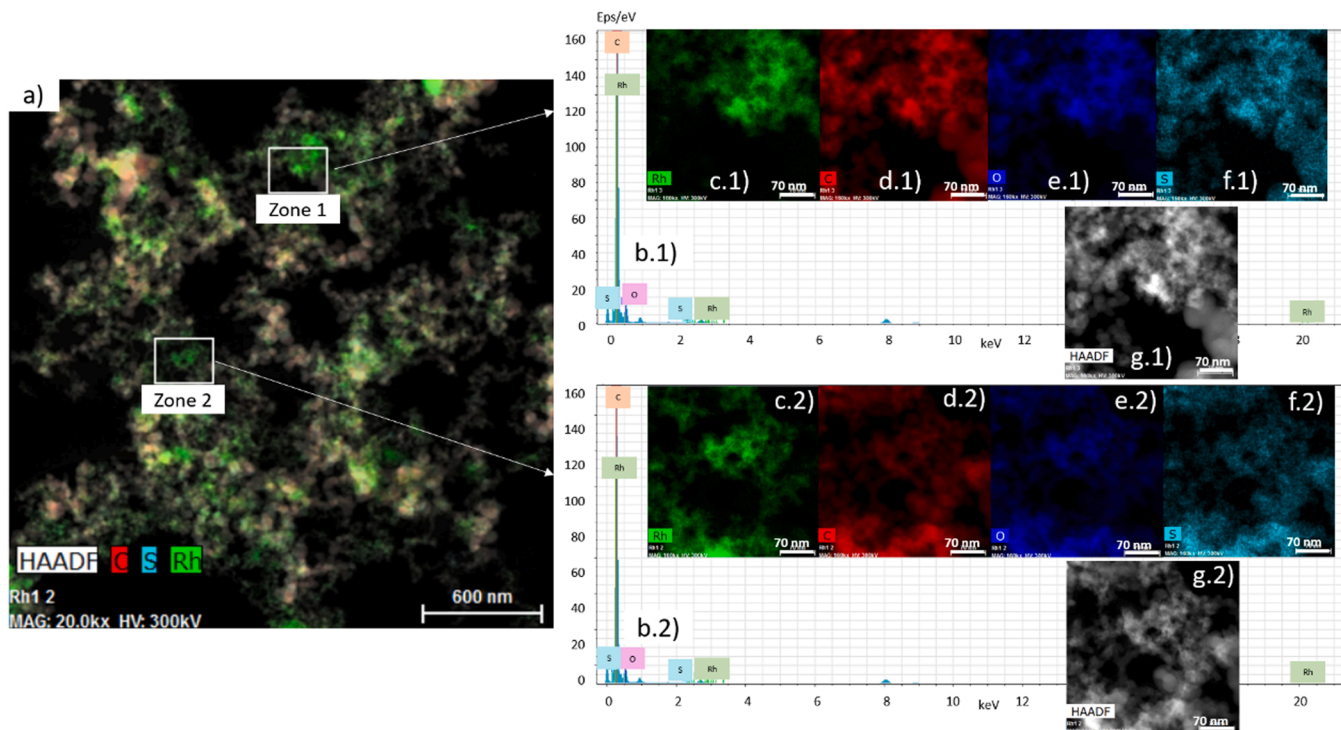

Fig. 4. (a) HAADF-STEM image, (b) EDX spectra and the corresponding elemental mapping images of (c) Rh, (d) C, (e) O, (f) S, and (g) HAADF images for two different Rh/C regions (Zone 1 and Zone 2).

provided with characteristics explained in Section 2.3. For this purpose, RDEs coated with a thin film of Rh/C electrocatalysts in Nafion were prepared. As compared to the voltammogram of a RDE coated only with oxidized Vulcan XC-72 and Nafion (Fig. 6), the voltammogram of a RDE coated with Rh/C and Nafion shows a redox process at about 0.05 V vs. RHE, which is ascribed to the two-electron two-proton reduction of the pyrazine moiety linking the Rh complex to Vulcan XC-72 [49]. This redox process is followed by the large reduction wave, which onsets at ca. -0.1 V and is ascribed to the catalysis of the HER. No limiting current corresponding to the kinetics of proton mass transport was observed in the investigated potential range, as expected under strongly acidic conditions (pH 1).

To determine the Tafel parameters of the HER in 0.1 M H_2SO_4, the current at a RDE (2000 rpm) coated with a thin film of Rh/Vulcan in Nafion upon consecutive potential steps for 100 s in the range -0.13 to -0.33 V vs. RHE was recorded as shown in Fig. 7. The calculated Tafel plot shows that the overpotential varies linearly with the logarithm of the current over more than one decade (dec) (Fig. S7 of the Supplementary Information). In the investigated potential range, the Tafel slope has a value of -177 mV·dec^{-1}, consistent with a mechanism involving a coupled proton electron transfer rate-determining step [49]. Extrapolation to zero over-potential gives an apparent exchange current density of $j_{0,geom} = 8.1 \times 10^{-6}$ A·cm^{-2}. As a result, we can estimate that the apparent HER activity of the Rh/C electrocatalyst at the over-potential of -50 mV and pH 1 is of the order of 0.015 mA·cm^{-2}. These results compare favorably with those reported for MoS-based electro-catalytic materials under similarly strong acidic conditions (pH < 1) and are significantly better than those reported for Co-N$_4$ based electro-catalysts [54]. Besides, normalized to the Rh loading, the mass activity for the HER of the Rh/C electrocatalyst at the overpotential of -50 mV and pH 1 is of the order of 34 mA·mg^{-1}. This value of mass activity is about 8 times smaller than that reported for a commercial Pt/C electrocatalyst under otherwise similar experimental conditions [47]. However, it is to be emphasized that commercial Pt/C electrocatalysts usually have a precious metal loading exceeding 10% in wt., whereas the Rh/C electrocatalysts used in this manuscript have a precious metal loading of only 0.4–0.5% in wt. We, therefore, argue that our approach, in which the active site is a single metal site with a well-controlled environment, could be successful to significantly decrease the amount of precious metal needed in the electrodes of the PEM electrolyzer.

3.3. Performance in the PEM electrolyzer

A commercial hydrogen electrolyzer was used to study the Rh/C

Fig. 7. Amperometric curves recorded at a RDE (2000 rpm) coated with oxidized Vulcan XC-72 and Nafion (blue trace) or Rh/C and Nafion (red trace) immersed in N$_2$-purged 0.1 M H$_2$SO$_4$ (pH 1). The potential was stepped to -0.13, -0.18, -0.23, -0.28 and -0.33 V vs RHE, respectively.

electrocatalyst synthesized and characterized previously. As explained above, in order to establish the performance of these materials in the PEM electrolyzer, two different Rh metal loadings (0.0044 and 0.0066 mg·cm^{-2}) were tested in GDEs to carry out the HER. In this way, different polarization curves were conducted in the range of $j_{,geom}$ from 0.04 to 0.48 mA·cm^{-2} (Fig. 8); the results are summarized in Tables S2 and S3 of the Supplementary Information.

The influence of the Rh/C-GDE loading (0.0044 and 0.0066 mg·cm^{-2}) was studied between 50 °C and 70 °C, which is the operating tem-perature range recommended by the manufacturer. Firstly, working with higher Rh loadings (0.0066 mg Rh·cm^{-2}) results in a better per-formance for the HER, reaching lower cell potentials for the same $j_{,geom}$, as depicted in Fig. 8. In fact, for a $j_{,geom}$ value of 0.04 mA·cm^{-2}, a po-tential value of 1.62 V for the Rh loading of 0.0066 mg Rh·cm^{-2}, while this potential value achieves a higher value (1.71 V) for the Rh loading of 0.0044 mg Rh·cm^{-2}.

Focusing on the cell potential, an increment, between the values of $j_{,geom}$ supplied to the single cell from 0.04 to 0.48 mA·cm^{-2}, using a loading of 0.0044 mg Rh·cm^{-2} implies an increase in the voltage, reaching values of 2.28 V at a $j_{,geom}$ of 0.48 A·cm^{-2}. On the other hand, the potential of the electrocatalyst with the highest loading (0.0066 mg Rh·cm^{-2}) leads to a small increase, specifically, 20% at both
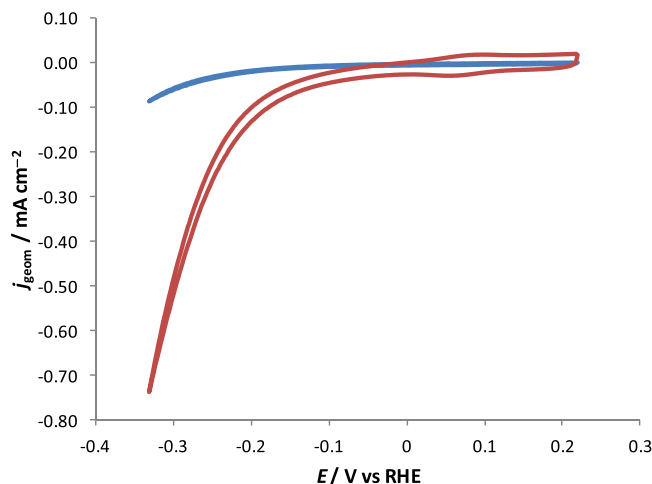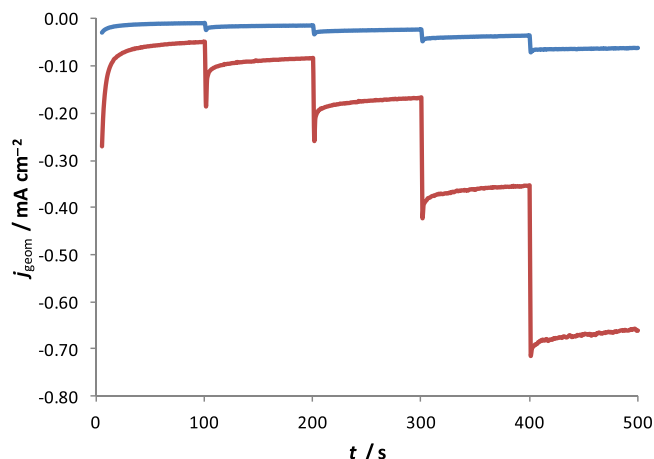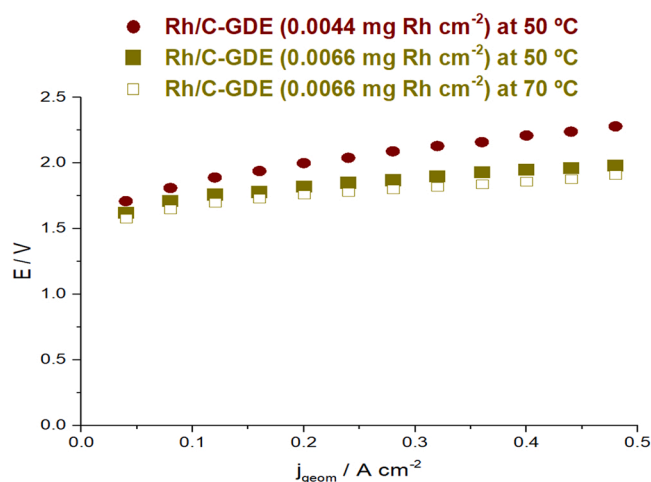

Fig. 6. Cyclic voltammograms (scan rate of 5 mV·s^{-1}) of an electrode coated with only oxidized Vulcan and Nafion (blue trace) and Rh/C electrocatalyst and Nafion (red trace) immersed in N$_2$-purged 0.1 M H$_2$SO$_4$ (pH 1).

Fig. 8. Polarization curves at 50 and 70 °C for the different Rh/C-GDEs load-ings (0.0044 and 0.0066 mg Rh·cm^{-2}) tested as cathodes to carry out the HER in a PEM electrolyzer.

temperatures (from ≈1.60 V to ≈1.95 V). A similar behavior was observed by Shiva Kumar et al. [34], who reported that the electrocatalytic activity of B-CNPs for the HER increases with increasing B-doping.

If we pay attention to the H_2 flow rate produced (values are provided as Supplementary Information) both Rh loadings achieve similar values of H_2 production in each value of the j_{geom} supplied to the single cell in a range from 10 (a supply of 0.04 A·cm^{-2}) to 78 mL·min^{-1} (a supply of 0.48 A·cm^{-2}). Obviously, the energy consumption will be lower in the case of 0.0066 mg·cm^{-2} loading because of the lesser cell potentials achieved in comparison with the loading of 0.0044 mg·cm^{-2}. In contrast, promising results have been obtained working at 70 °C (Fig. 8) for the Rh/C-GDE 0.0066 mg·cm^{-2} loading due to the lower potentials for the same j_{geom} in the polarization curves to carry out the HER in the PEM electrolyzer.

Another essential point to be considered is the fact that the Rh/C electrocatalysts employed in this work do not suffer any degradation during the experiments and provide similar results with the same GDE, and replicating comparable behaviors with different electrodes. Thus, the process is stable, repetitive and the GDE procedure fabrication is robust, effective, and environmentally friendly.

3.4. Comparison with commercial electrocatalysts

In this section, the behavior of the synthesized Rh/C electrocatalyst presented in this work is compared to other commercial CPt/C-GDE (commercial Pt electrocatalysts), Pt/C-MEA and Pt/C-GDE (commercial cathodes) fabricated with a catalytic loading of 0.3, 0.3 and 0.4 mg Pt·cm^{-2}, respectively, at 70 °C. It is important to highlight that the comparison was performed with the Rh/C-GDE loading of 0.0066 mg·cm^{-2}, which offers the best performance to carry out the HER in the PEM electrolyzer.

The polarization curves obtained for each cathode are illustrated in Fig. 9. Comparing both Pt-GDEs, the electrodes showed similar results, especially at lower density j_{geom}, demonstrating that the procedure of synthesis presented in this work is suitable for the preparation of GDEs. This point is crucial because the Pt/C-GDE fabricated in this work and the Pt/C-MEA contain 0.3 mg Pt·cm^{-2} that is 1.3 times lower than the loading of commercial Pt/C-GDEs that are 0.4 mg Pt·cm^{-2}. Besides, the trend and the values achieved working with commercial GDEs and MEAs based on Pt/C and with the Rh/C-GDE are pretty similar (results differed by 10% at most), demonstrating that the use of Rh-based materials supposes a step forward in the development of high-effective electrocatalysts. This point is crucial because the Rh/C-GDE metal loading is 60 times lower than the loading of Pt/C commercial electrodes. Therefore,
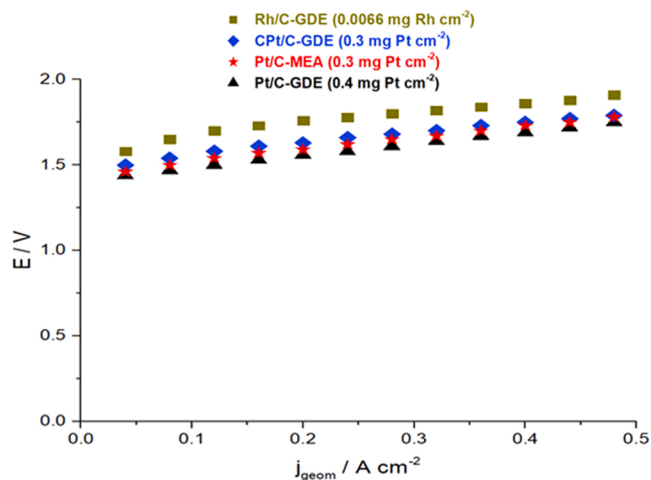
the slight difference between the polarization curves is attributed to the much higher loadings of Pt-based electrodes.

In this context, as mentioned above, Holzapfel et al. [31] reported voltage values of 1.85 V for a current density of 0.5 A·cm^{-2}, by using cathodes made of Mo_3S_{13} clusters supported on nitrogen-doped carbon nanotubes, but in this case, the catalyst loading was 3 mg·cm^{-2}, 450 times higher than the value used in the current work. Mo et al. [25] also described voltage values of around 1.6 V and 2.1 V for current densities of 0.5 A·cm^{-2}, when studying the performance of transition metal atom-doped monolayer MoS_2 as cathode, but also with higher catalyst loadings than those applied in this work, 4.5 mg·cm^{-2} instead of 0.0066 mg Rh·cm^{-2}. Shi et al. [32] by using $Ni_{12}P_5$-Ni_2PSo as a cathode reported a voltage value of around 1.8 V (0.5 A·cm^{-2}) when a catalyst loading of 16.6 mg·cm^{-2} was applied, while in the present study the achieved voltage is 1.91 V. Thus, these results constitute a step forward in the search for new catalysts competitive with conventional Pt-based electrodes since the electrocatalysts presented in this work are more sustainable, environmentally friendly, and avoid the poisoning of Pt-based electrocatalysts.

Attending to hydrogen production, the results are shown in Fig. 10, recalling the fact that the polarization curves are intimately linked with this Figure. This Figure depicts the different voltages required as a function of the j_{geom} for different H_2 flow rates, between 10 and 78 mL per minute. As can be seen, the results revealed that the employment of Rh/C-GDE requires more voltage, as expected. In this way, the main reason is that the use of this electrocatalyst implies higher energy consumption, especially when the density currents supplied are higher than 0.2 A·cm^{-2}. On the contrary, when loading of 0.0066 mg·cm^{-2} of Rh metal electrocatalyst was employed, at elevated j_{geom}, the results were highly competitive when compared to the commercial Pt cathode (Pt/C-MEA), which offers the best performance since the voltage required is the minimum value in all cases.

4. Conclusions

In summary, this work reports a robust synthesis procedure and a complete characterization of new electrodes that are synthesized by grafting a Rh-based organometallic complex (i.e. RhCp*Cl(phendiamine)Cl) on oxidized carbon black support through a strong pyrazine link to significantly decrease the amount of precious metal. The hydrogen evolution reaction was efficiently catalyzed at Rh-based cathode in which the metal loadings are in the range of 3.2 and
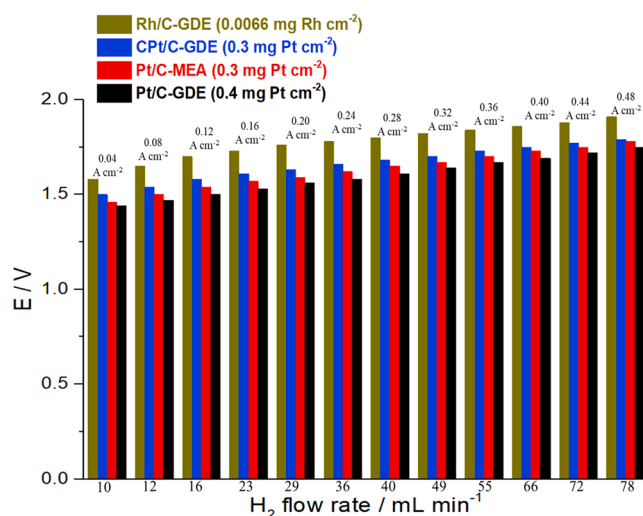

Fig. 9. Polarization curves for the different cathodes tested to carry out the HER in a PEM electrolyzer at 70 ºC.

Fig. 10. H_2 production (mL·min^{-1}) as a function of the voltage (V) and the geometric current density (mA·cm^{-2}) at 70 °C for the different cathodes tested to carry out the HER in a PEM electrolyzer.

4.7 mg·g^{-1}. The activity of Rh/C for the electrocatalysis of the HER in acid solution (pH 1) was first evaluated using the RDE technique. From the Tafel plot analysis, the mass activity results in a value of 34 mA·mgRh^{-1} at an overpotential of -50 mV, competitive with that achieved by MoS-based electrocatalysts. Importantly, Rh/C is found to be stable under electrocatalytic conditions at pH 1, emphasizing the strength of the pyrazine link between the Rh center and the carbon surface. Finally, the performance of Rh/C electrocatalysts is evaluated in a commercial PEM electrolyzer to carry out the HER, showing promising results despite the ultra-low metal loading when compared to other Pt-based cathodes. In this context, the employment of a Rh/C-GDE loading of 0.0066 mg Rh·cm^{-2} represents a step forward in the search of new cost-effective electrocatalysts to carry out the HER since similar results in terms of energy consumption (as a function of the cell potential and the geometric current density) and hydrogen production are obtained in comparison with Pt/C commercial GDEs. In terms of voltage, employing the Rh/C-GDE (0.0066 mg Rh·cm^{-2}) increases from 1.60 V using a j$_{geom}$ of 0.04 A·cm^{-2} to 1.95 V working with j$_{geom}$ of 0.48 A·cm^{-2}. These values are in accordance with most of the literature reported until the moment. Thus, this manuscript positions the use of ultra-low loading Rh-based materials in a preferential place to catalyze the HER in a PEM electrolyzer since they have similar activity as Pt, and simultaneously, this material is less sensitive to poisoning than Pt-based electrocatalysts.

CRediT authorship contribution statement

Gema Pérez: Methodology, Investigation, Data curation, Writing – original draft, Validation. **Guillermo Díaz-Sainz:** Writing – original draft, Investigation, Visualization. **Lucía Gómez-Coma:** Writing – original draft, Investigation, Visualization. **Lucía Álvarez-Miguel:** Methodology, Investigation, Validation. **Aymeric Garnier:** Investigation, Data curation. **Nolwenn Cabon:** Investigation, Data curation. **Alfredo Ortiz:** Conceptualization, Writing – original draft, Writing – review & editing, Resources, Supervision, Project administration, Funding acquisition. **Frederic Gloaguen:** Writing – review & editing, Resources, Supervision, Funding acquisition. **Inmaculada Ortiz:** Writing – review & editing, Resources, Supervision, Funding acquisition.

Declaration of Competing Interest

The authors declare that they have no known competing financial interests or personal relationships that could have appeared to influence the work reported in this paper.

Acknowledgements

Appendix A. Supporting information

Supplementary data associated with this article can be found in the online version at doi:10.1016/j.jece.2022.107682.

References

[1] J. Lelieveld, K. Klingmüller, A. Pozzer, R.T. Burnett, A. Haines, V. Ramanathan, Effects of fossil fuel and total anthropogenic emission removal on public health and climate, Proc. Natl. Acad. Sci. U. S. A 116 (2019) 7192–7197, https://doi.org/10.1073/pnas.1819989116.

[2] R. Ortiz-Imedio, A. Ortiz, J.C. Urroz, P.M. Diéguez, D. Gorri, L.M. Gandía, I. Ortiz, Comparative performance of coke oven gas, hydrogen and methane in a spark ignition engine, Int. J. Hydrog. Energy 46 (2020) 17572–17586, https://doi.org/10.1016/j.ijhydene.2019.12.165.

[3] Glasgow Climate Change Conference – October-November 2021 | CMNUCC, (n.d.). ⟨https://unfccc.int/es/node/307746⟩ (accessed December 23, 2021).

[4] R. Muntean, D.T. Pascal, U. Rost, G. Mărginean, M. Brodmann, N. Vaszilcsin, Synthesis and characterisation of platinum–cobalt–manganese ternary alloy catalysts supported on carbon nanofibers: An alternative catalyst for hydrogen evolution reaction, Int. J. Hydrog. Energy 45 (2020) 26217–26225, https://doi.org/10.1016/j.ijhydene.2020.02.041.

[5] A. Pareek, R. Dom, J. Gupta, J. Chandran, V. Adepu, P.H. Borse, Insights into renewable hydrogen energy: Recent advances and prospects, Mater. Sci. Energy Technol. 3 (2020) 319–327, https://doi.org/10.1016/j.mset.2019.12.002.

[6] N. Karikalan, P. Sundaresan, S.M. Chen, R. Karthik, C. Karuppiah, Cobalt molybdenum sulfide decorated with highly conductive sulfur-doped carbon as an electrocatalyst for the enhanced activity of hydrogen evolution reaction, Int. J. Hydrog. Energy 44 (2019) 9164–9173, https://doi.org/10.1016/j.ijhydene.2019.02.110.

[7] B. Anzelmo, J. Wilcox, S. Liguori, Hydrogen production via natural gas steam reforming in a Pd-Au membrane reactor. Comparison between methane and natural gas steam reforming reactions, J. Memb. Sci. 568 (2018) 113–120, https://doi.org/10.1016/j.memsci.2018.09.054.

[8] L. García, Hydrogen production by steam reforming of natural gas and other nonrenewable feedstocks, Compendium of hydrogen energy, Hydrog. Prod. Purif. Woodhead Publ. Ser. Energy (2015) 83–107, https://doi.org/10.1016/b978-1-78242-361-4.00004-2.

[9] S. Sangrola, A. Kumar, S. Nivedhitha, J. Chatterjee, S. Subbiah, S. Narayanasamy, Optimization of backwash parameters for hollow fiber membrane filters used for water purification, J. Water Supply Res. Technol. AQUA 69 (2020) 523–537, https://doi.org/10.2166/aqua.2020.079.

[10] I. Lucentini, A. Casanovas, J. Llorca, Catalytic ammonia decomposition for hydrogen production on Ni, Ru and Ni[sbnd]Ru supported on CeO$_2$, Int. J. Hydrog. Energy 44 (2019) 12693–12707, https://doi.org/10.1016/j.ijhydene.2019.01.154.

[11] Z. Fan, W. Weng, J. Zhou, D. Gu, W. Xiao, Catalytic decomposition of methane to produce hydrogen: A review, J. Energy Chem. 58 (2021) 415–430, https://doi.org/10.1016/j.jechem.2020.10.049.

[12] M. Muresan, C.C. Cormos, P.S. Agachi, Techno-economical assessment of coal and biomass gasification-based hydrogen production supply chain systems, Chem. Eng. Res. Des. 91 (2013) 1527–1541, https://doi.org/10.1016/j.cherd.2013.02.018.

[13] J. Corredor, D. Harankahage, F. Gloaguen, M.J. Rivero, M. Zamkov, I. Ortiz, Influence of QD photosensitizers in the photocatalytic production of hydrogen with biomimetic [FeFe]-hydrogenase. Comparative performance of CdSe and CdTe, Chemosphere 278 (2021) 130485, https://doi.org/10.1016/j.chemosphere.2021.130485.

[14] J. Corredor, M.J. Rivero, C.M. Rangel, F. Gloaguen, I. Ortiz, Comprehensive review and future perspectives on the photocatalytic hydrogen production, J. Chem. Technol. Biotechnol. 94 (2019) 3049–3063, https://doi.org/10.1002/jctb.6123.

[15] A.A. Cullen, K. Heintz, L. O'Reilly, C. Long, A. Heise, R. Murphy, J. Karlsson, E. Gibson, G.M. Greetham, M. Towrie, M.T. Pryce, A time-resolved spectroscopic investigation of a novel BODIPY copolymer and its potential use as a photosensitiser for hydrogen evolution, Front. Chem. 8 (2020), 584060, https://doi.org/10.3389/fchem.2020.584060.

[16] X. Gu, X. Yang, L. Feng, An efficient RuTe2/Graphene catalyst for electrochemical hydrogen evolution reaction in acid electrolyte, Chem. Asian J. 15 (2020) 2886–2891, https://doi.org/10.1002/asia.202000734.

[17] D.S. Falcão, A.M.F.R. Pinto, A review on PEM electrolyzer modelling: Guidelines for beginners, J. Clean. Prod. 261 (2020), 121184, https://doi.org/10.1016/j.jclepro.2020.121184.

[18] F.M. Sapountzi, J.M. Gracia, C.J. (Kees-Jan) Weststrate, H.O.A. Fredriksson, J. W. (Hans) Niemantsverdriet, Electrocatalysts for the generation of hydrogen, oxygen and synthesis gas, Prog. Energy Combust. Sci. 58 (2017) 1–35, https://doi.org/10.1016/j.pecs.2016.09.001.

[19] E. López-Fernández, C.G. Sacedón, J. Gil-Rostra, F. Yubero, A.R. González-Elipe, A. de Lucas-Consuegra, Recent advances in alkaline exchange membrane water electrolysis and electrode manufacturing, Mol Vol. 26 (2021) 6326, https://doi.org/10.3390/MOLECULES26216326.

[20] K. Kamlungsua, P.C. Su, S.H. Chan, Hydrogen generation using solid oxide electrolysis cells, Fuel Cells 20 (2020) 644–649, https://doi.org/10.1002/fuce.202070602.

[21] M. Carmo, D.L. Fritz, J. Mergel, D. Stolten, A comprehensive review on PEM water electrolysis, Int. J. Hydrog. Energy 38 (2013) 4901–4934, https://doi.org/10.1016/j.ijhydene.2013.01.151.

[22] H. Kim, H. Park, H. Oh, S.K. Kim, Facile electrochemical preparation of nonprecious Co-Cu alloy catalysts for hydrogen production in proton exchange membrane water electrolysis, Int. J. Energy Res. 44 (2020) 2833–2844, https://doi.org/10.1002/er.5099.

[23] S. Shiva Kumar, V. Himabindu, Hydrogen production by PEM water electrolysis – A review, Mater. Sci. Energy Technol. 2 (2019) 442–454, https://doi.org/10.1016/j.mset.2019.03.002.

[24] S. Anwar, F. Khan, Y. Zhang, A. Djire, Recent development in electrocatalysts for hydrogen production through water electrolysis, Int. J. Hydrog. Energy 46 (2021) 32284–32317, https://doi.org/10.1016/j.ijhydene.2021.06.191.

[25] J. Mo, S. Wu, T.H.M. Lau, R. Kato, K. Suenaga, T.S. Wu, Y.L. Soo, J.S. Foord, S.C. E. Tsang, Transition metal atom–doped monolayer MoS₂ in a proton-exchange membrane electrolyzer, Mater. Today Adv. 6 (2020) 1020, https://doi.org/10.1016/j.mtadv.2019.100020.

[26] S. Shiva Kumar, S.U.B. Ramakrishna, B. Rama Devi, V. Himabindu, Phosphorus-doped graphene supported palladium (Pd/PG) electrocatalyst for the hydrogen evolution reaction in PEM water electrolysis, Int. J. Green. Energy 15 (2018) 558–567, https://doi.org/10.1080/15435075.2018.1508468.

[27] J. Chi, H. Yu, Water electrolysis based on renewable energy for hydrogen production, Cuihua Xuebao/Chin. J. Catal. 39 (2018) 390–394, https://doi.org/10.1016/S1872-2067(17)62949-8.

[28] H. Wu, C. Feng, L. Zhang, J. Zhang, D.P. Wilkinson, Non-noble metal electrocatalysts for the hydrogen evolution reaction in water electrolysis, Electrochem. Energy Rev. 4 (2021) 473–507, https://doi.org/10.1007/s41918-020-00086-z.

[29] S. Wang, A. Lu, C.J. Zhong, Hydrogen production from water electrolysis: Role of catalysts, Nano Converg. 8 (2021) 4, https://doi.org/10.1186/s40580-021-00254-x.

[30] Y. Ma, G. Guan, X. Hao, J. Cao, A. Abudula, Molybdenum carbide as alternative catalyst for hydrogen production – A review, Renew. Sustain. Energy Rev. 75 (2017) 1101–1129, https://doi.org/10.1016/j.rser.2016.11.092.

[31] P.K.R. Holzapfel, M. Bühler, D. Escalera-López, M. Bierling, F.D. Speck, K.J. J. Mayrhofer, S. Cherevko, C.V. Pham, S. Thiele, Fabrication of a robust PEM water electrolyzer based on non-noble metal cathode catalyst: [Mo₃S₁₃]²⁻ clusters anchored to N-Doped carbon nanotubes, Small 16 (2020), 2003161, https://doi.org/10.1002/smll.202003161.

[32] H. Shi, Q. Yu, G. Liu, X. Hu, Promoted electrocatalytic hydrogen evolution performance by constructing Ni₁₂P₅–Ni₂P heterointerfaces, Int. J. Hydrog. Energy 46 (2021) 17097–17105, https://doi.org/10.1016/j.ijhydene.2021.02.159.

[33] S. Shiva Kumar, S.U.B. Ramakrishna, K. Naga Mahesh, B. Rama Devi, V. Himabindu, Palladium supported on phosphorus–nitrogen dual-doped carbon nanoparticles as cathode for hydrogen evolution in PEM water electrolysis, Ion. (Kiel.) 25 (2019) 2615–2625, https://doi.org/10.1007/s11581-018-2783-0.

[34] S. Shiva Kumar, V. Himabindu, Boron-doped carbon nanoparticles supported palladium as an efficient hydrogen evolution electrode in PEM water electrolysis, Renew. Energy 146 (2020) 2281–2290, https://doi.org/10.1016/j.renene.2019.08.068.

[35] M. Smiljanić, Z. Rakočević, S. Štrbac, Electrocatalysis of hydrogen evolution reaction on tri-metallic Rh@Pd/Pt(poly) electrode, Int. J. Hydrog. Energy 43 (2018) 2763–2771, https://doi.org/10.1016/j.ijhydene.2017.12.112.

[36] L.W. Chen, H.W. Liang, Ir-based bifunctional electrocatalysts for overall water splitting, Catal. Sci. Technol. 11 (2021) 4673–4689, https://doi.org/10.1039/d1cy00650a.

[37] M. Sarno, E. Ponticorvo, High hydrogen production rate on RuS₂@MoS₂ hybrid nanocatalyst by PEM electrolysis, Int. J. Hydrog. Energy 44 (2019) 4398–4405, https://doi.org/10.1016/j.ijhydene.2018.10.229.

[38] P. Paunović, D.S. Gogovska, O. Popovski, A. Stoyanova, E. Slavcheva, E. Lefterova, P. Iliev, A.T. Dimitrov, S.H. Jordanov, Preparation and characterization of Co-Ru/TiO₂/MWCNTs electrocatalysts in PEM hydrogen electrolyzer, Int. J. Hydrog. Energy 36 (2011) 9405–9414, https://doi.org/10.1016/j.ijhydene.2011.04.014.

[39] Z. Han, R.L. Zhang, J.J. Duan, A.J. Wang, Q.L. Zhang, H. Huang, J.J. Feng, Platinum-rhodium alloyed dendritic nanoassemblies: An all-pH efficient and stable electrocatalyst for hydrogen evolution reaction, Int. J. Hydrog. Energy 45 (2020) 6110–6119, https://doi.org/10.1016/j.ijhydene.2019.12.155.

[40] J. Bai, X. Xiao, Y.Y. Xue, J.X. Jiang, J.H. Zeng, X.F. Li, Y. Chen, Bimetallic platinum-rhodium alloy nanodendrites as highly active electrocatalyst for the ethanol oxidation reaction, ACS Appl. Mater. Interfaces 10 (2018) 19755–19763, https://doi.org/10.1021/acsami.8b05422.

[41] Y. Kang, Q. Xue, P. Jin, J. Jiang, J. Zeng, Y. Chen, Rhodium nanosheets-reduced graphene oxide hybrids: A highly active platinum-alternative electrocatalyst for the methanol oxidation reaction in alkaline media, ACS Sustain. Chem. Eng. 5 (2017) 10156–10162, https://doi.org/10.1021/acssuschemeng.7b02163.

[42] J. Lu, L. Zhang, S. Jing, L. Luo, S. Yin, Remarkably efficient PtRh alloyed with nanoscale WC for hydrogen evolution in alkaline solution, Int. J. Hydrog. Energy 42 (2017) 5993–5999, https://doi.org/10.1016/j.ijhydene.2017.01.181.

[43] Y. Zhao, J. Bai, X.R. Wu, P. Chen, P.J. Jin, H.C. Yao, Y. Chen, Atomically ultrathin RhCo alloy nanosheet aggregates for efficient water electrolysis in broad pH range, J. Mater. Chem. A. 7 (2019) 16437–16446, https://doi.org/10.1039/c9ta05334d.

[44] M.K. Kundu, R. Mishra, T. Bhowmik, S. Barman, Rhodium metal-rhodium oxide (Rh-Rh₂O₃) nanostructures with Pt-like or better activity towards hydrogen evolution and oxidation reactions (HER, HOR) in acid and base: correlating its HOR/HER activity with hydrogen binding energy and oxophilicity of the cat, J. Mater. Chem. A. 6 (2018) 23531–23541, https://doi.org/10.1039/c8ta07028h.

[45] H. Duan, D. Li, Y. Tang, Y. He, S. Ji, R. Wang, H. Lv, P.P. Lopes, A.P. Paulikas, H. Li, S.X. Mao, C. Wang, N.M. Markovic, J. Li, V.R. Stamenkovic, Y. Li, High-performance Rh₂P electrocatalyst for efficient water splitting, J. Am. Chem. Soc. 139 (2017) 5494–5502, https://doi.org/10.1021/jacs.7b01376.

[46] C. Zhu, S. Fu, Q. Shi, D. Du, Y. Lin, Single-atom electrocatalysts, Angew. Chem. Int. Ed. 56 (2017) 13944–13960, https://doi.org/10.1002/anie.201703864.

[47] N. Cheng, S. Stambula, D. Wang, M.N. Banis, J. Liu, A. Riese, B. Xiao, R. Li, T. K. Sham, L.M. Liu, G.A. Botton, X. Sun, Platinum single-atom and cluster catalysis of the hydrogen evolution reaction, Nat. Commun. 7 (2016) 13638, https://doi.org/10.1038/ncomms13638.

[48] M.K. Samantaray, V. D'Elia, E. Pump, L. Falivene, M. Harb, S. Ould Chikh, L. Cavallo, J.-M. Basset, The comparison between single atom catalysis and surface organometallic catalysis, Chem. Rev. 120 (2020) 734–813, https://doi.org/10.1021/acs.chemrev.9b00238.

[49] M.N. Jackson, C.J. Kaminsky, S. Oh, J.F. Melville, Y. Surendranath, Graphite conjugation eliminates redox intermediates in molecular electrocatalysis, J. Am. Chem. Soc. 141 (2019) 14160–14167, https://doi.org/10.1021/jacs.9b04981.

[50] A.F. Gullá, L. Gancs, R.J. Allen, S. Mukerjee, Carbon-supported low-loading rhodium sulfide electrocatalysts for oxygen depolarized cathode applications, Appl. Catal. A Gen. 326 (2007) 227–235, https://doi.org/10.1016/j.apcata.2007.04.013.

[51] U. Kölle, M. Grützel, Organometallic Rhodium(III) complexes as catalysts for the photoreduction of protons to hydrogen on colloidal TiO₂, Angew. Chem. Int. Ed. Engl. 26 (1987) 567–570, https://doi.org/10.1002/anie.198705671.

[52] F. Gloaguen, F. Andolfatto, R. Durand, P. Ozil, Kinetic study of electrochemical reactions at catalyst-recast ionomer interfaces from thin active layer modelling, J. Appl. Electrochem. 24 (1994) 863–869, https://doi.org/10.1007/BF00348773.

[53] NIST X-ray Photoelectron Spectroscopy Database. ⟨https://srdata.nist.gov/xps/⟩, 2022 (accessed 08 March 2022).

[54] S. Rioual, B. Lescop, F. Quentel, F. Gloaguen, A molecular material based on electropolymerized cobalt macrocycles for electrocatalytic hydrogen evolution, Phys. Chem. Chem. Phys. 17 (2015) 13374–13379, https://doi.org/10.1039/C5CP01210D.